ENHANCEMENT OF SUPERCONDUCTING PROPERTIES OF MgB$_2$ SUPERCONDUCTOR BY DOPING OF NANO-ALUMINA AND NANO-CARBON

K Shaikh[*1,2] , M. Shahabuddin[2], I A. Ansari[2], and N. S. Alzayed[2],

[1] Research Scholar, Singhania University, Jhunjhunu, Rajasthan, India.
2 Department of Physics, College of Science, King Saud University, Riyadh, Saudi Arabia

Abstract - The importance of MgB$_2$ lies in its simple crystal structure, relatively high T$_C$ (39K), low cost, large coherence length and transparency of grain boundaries to current flow. Systematic preparation of a series of bulk MgB$_2$ samples of Mg$_{1-x}$Al$_x$(B$_{1-y}$C$_y$)$_2$, x=2% ; y = 0%,1%,2%, 3%, 4%,6%, 10%, were carried out on nano alumina MgB$_2$ co-doped with nano carbon. Bulk MgB$_2$ samples have prepared by standard solid-state reaction method, followed by ball milling. As the concentration of nano carbon doped MgB$_2$ increases their resistivity increases accordingly, results the lowering of transition temperature, T$_c$. Here, we report that co-doping play an important role in decreasing the lattice parameters. A systematical comparison of nano alumina and nano carbon doped MgB$_2$ with structure; superconducting transition, resistivity and dc-susceptibility are discussed. Keeping this in mind we investigated the effect of simultaneous doping of nano Al and nano C in different ratio on J$_C$ around 20K. We found more than one order of increase in J$_C$ at 20K in 4.8 T field for particular ratio of Al and C.

Keyword - MgB$_2$, nano-Alumina, nano-carbon, co-doped, superconductivity, critical current.

INTRODUCTION

Since 2001, the discovery of superconductivity at 39 K in MgB$_2$ has initiated an interest of activity aimed to understanding the origin of the large superconducting transition temperature (T$_c$) [1]. MgB$_2$ is composed of two elements, magnesium and boron. MgB$_2$ have high upper critical field H$_{c2}$, high irreversibility H$_{irr}$, low material cost and enables to be used at the cryocooler temperature.

A number of groups undertook synthesis and characterization of (Mg$_{1-x}$W$_x$)B$_2$ or Mg(B$_{1-y}$Z$_y$)$_2$ (W = transition metal, Li, Be, Al []; Z = C, Si []) materials. Carbon substitution was reported in several reports [2–7]. Almost all substitutions have led to a decrease in T$_c$ with an exception of Zn [8], which shows no change even for 30% substitution. As a simple and practical method, chemical doping seems to be a promising technique for improving the critical current density J$_c$(H). Especially, carbon-containing precursors, such as SiC, graphite, nanocarbon (NC), and carbon nanotubes (CNTs), were found to be effective for the enhancement of the irreversibility field (H$_{irr}$) and J$_c$(H), because the substitution of C into B site leads to intra-band scattering that increases the H$_{c2}$, as reported by many groups [9–12]. Among these precursors, we considered that nano carbon would be an effective dopant, because of its nano size and low decomposition temperature from 150 ˚C to 750 ˚C. Slusky et al. [13] have shown that Al can aggressively react with MgB$_2$ and the substitution into the Mg position leads to a loss of superconductivity.

Indeed, C as well as Al introduces extra electrons into the conduction bands of MgB$_2$. This leads to a reduction of the hole density-of-states of the most important σ-band, and it causes the suppression of T$_c$ and superconducting gaps in both series of doped systems [14]. Although Al-oxide-doped MgB$_2$ has been studied [15] but the effect of nano-alumina oxide as well as nano carbon addition on the properties of MgB$_2$ has not been reported within our knowledge. In the present work, we study the effect of co-doping of nano-alumina oxide and nano carbon into bulk MgB$_2$ by Mg$_{1-x}$ Al$_x$ (B$_{1-y}$C$_y$)$_2$ formula.

EXPERIMENTAL DETAILS

In the present study we prepared a series of seven samples of Mg$_{1-X}$Al$_X$(B$_{1-y}$ C$_y$)$_2$ pure, where x is 0 and .02 while y varies from .01 to .06. That means we have a pure MgB$_2$, 2% Al doped MgB$_2$ and five samples with co Al and C doped in which C varies 1 to 6% and Al fixed to 2%. These samples were prepared using standard solid state reaction method in which constituent materials were mixed in stoichiometric ratio. The constituent materials were 99.99% amorphous boron powder (Sigma Aldrich), 99.9% Mg powder (CERAC with average particle size 45 nm), 99.9% nano amorphous C, and, 99.9% Al2O3 both nano powder from Sigma Aldrich. These were mixed using planetary ball milling machine for 8 hours under 150 rpm. After the ball milling, the powder was pelletized under 10 tons of the pressure. During pellet preparation equal amounts of the powder were used to have equal size of pellets. These were then wrapped in the tantalum foil and placed in a cylindrical crucible of soft iron.

Crucibles were placed inside a long quartz tube closed at one end and valve fitted at the other end for evacuation. The quartz tube was evacuated to the order of 10^{-5} torr. It was placed inside the preheated furnace. All seven samples were sintered at 750 °C for two hours under high vacuum under same conditions and finally furnace cooled.

The crystalline structure analysis was investigated by powder X-ray diffraction (XRD) using an X'pert MRD diffractometer with CuKα radiation at room temperature. Resistance of the samples was measured by in-house made resistivity measurement system using the standard four probe method. Temperature dependence of resistivity was determined from 12 K to 300 K using closed cycle He refrigerator. The dc-susceptibility was measured by in-house made susceptometer. The DC magnetizations of these samples were measured using a PAR-4500 Vibrating Sample Magnetometer (VSM). Temperature was monitored using a C-glass thermometer with accuracy better than 0.05 K. The weights of all the samples used in the present study were kept at 45–55 mg. For VSM measurements all samples were cut into 8x2.5x2 mm rectangular shape to avoid the shape effect in comparison of different samples The irreversibility field *(H*irr*)* is obtained from the lowest magnetic field at which the magnetization is reversible.

RESULT AND DISCUSSION

Figure 1 show XRD pattern of $\{(Mg_{1-x}Al_x) + (B_{1-y}C_y)_2\}$, samples where x = 2%, and y = 0%, 2%,3%, 4%, 6%, 10%. Note that there are no peak related to nano carbon in XRD pattern of nano Carbon and Al oxide co-doped bulk due to the amorphous nano carbon and nano Aluminum oxide powder used. Minority phase MgO is detected. It clearly shows that there is only MgB_2 phase with minor trace of MgO and un-reacted Mg. in pure MgB2 samples the un-reacted Mg is negligible but C0% and C6% having more percentage of un-reacted Mg.
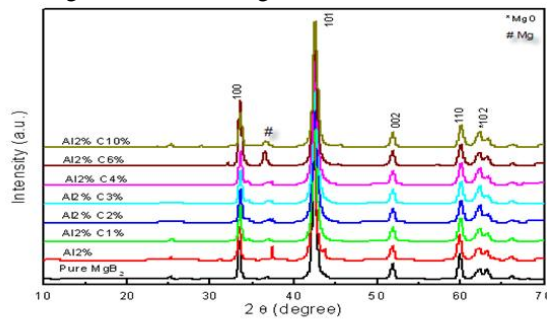

Fig 1. X-ray diffraction pattern for $\{(Mg_{1-x}Al_x) + (B_{1-y}C_y)_2\}$, with x = 2%, and y = 0%, 2%,3%, 4%, 6%, 10%,

This has been further verified by measuring the electrical resistivity of all samples as a function of temperature which is shown in Fig.2. From the figure it is clear that the normal state resistivity of pure, 0%, 2% 4% and 6% doped samples is nearly the same. There is significant change in the normal state resistivity of 10% in comparison to that of pure. This might be due to void or impurity phase MgO at grain boundary. The substitution is further confirmed from the change in the T_C of the doped samples as shown in the of Fig.2.
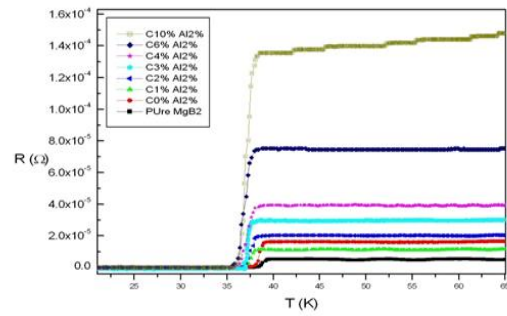

Fig2. The Temperature dependent of electrical resistivity of $\{(Mg_{1-x}Al_x) + (B_{1-y}C_y)_2\}$, with x = 2%, and y = 0%, 2%,3%, 4%, 6%, 10%.

The value of delta Tc measure from Fig 1 according to which has been tabulated in table 1. The value of delta Tc does significantly change with doping concentration Nano carbon and nano alumina is divalent as Mg so it does not affect the carrier density in B-plane.and at the same time it is at Mg site so its interaction with the conducting B-plane is very weak. Higher delta Tc measure in C0% and Al2% doped samples and less value in C3% and Al 2% doped sample.

Samples	Onset T(K)	Tc	ΔT= T-Tc
Pure MgB₂	39.56	35.87	3.69
C0% Al2%	39.37	27.94	11.43
C1% Al2%	38.03	32.85	5.18
C2% Al2%	38.62	36.3	2.32
3% Al2%	38.28	37.03	1.25
C4% Al2%	38.83	35.53	3.3
C6% Al2%	38.43	35.29	3.14
C10% Al2%	38.3	35.66	2.64

Table1 Resistivity comparison for $\{(Mg_{1-x}Al_x) + (B_{1-y}C_y)_2\}$, with x = 2%, and y = 0%, 2%,3%, 4%, 6%, 10%.

The Full Widths at Half Maximum (FWHM) were determined with the program PowderX by using x-ray diffraction data. These FWHM data were used to evaluate the grain size and strain of different doped samples using the Williamson and Hall model [42]:

$$FWHM \; x \; \cos(\theta) = \frac{0.94\lambda}{(Grain\,size)} + 4 \; x \; Strain \; x \; \sin(\theta)$$

where λ is the wavelength of monochromatic CuKα radiation (1.540598 Å) and θ is the angle of peak position at x-ray plot. The above relation encompasses the combination of Scherrer equation for size broadening and Stokes and Wilson expression for strain broadening. After plotting the FWHM x cos(θ) vs. sin(θ) as shown in the figure 3 and fitting the straight line.
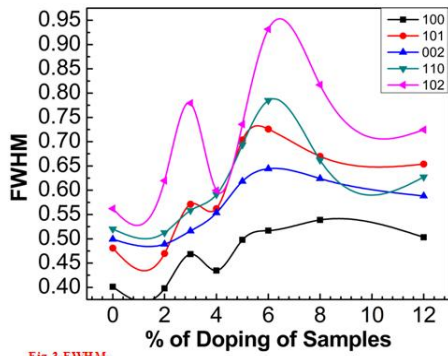
Fig.3 FWHM

The *a* parameter is shown in Fig.4 which clearly depict that the Al doping does not affect the lattice constant *a*. while at the same time it is decreasing the c parameter this confirm that Al has gone to Mg site. The parameter, *a,* is decreasing very fast with respect to increase in C concentration. This indicates the substitution of C has taken place in the basal plane of MgB_2 i.e in the Boron plane.
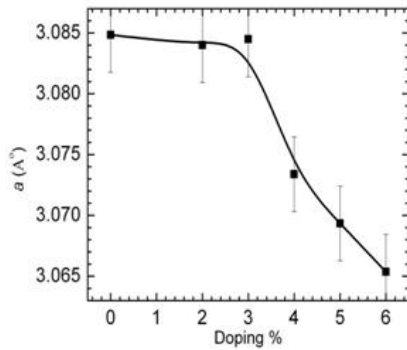

Fig. 4. *a* parameter of Al-C co-doped $Mg_{1-x}Al_x(B_{1-y}C_y)_2$ superconductors as function of total doping % C and Al.

From Fig 5 it is clear that the Al doping decreases the *c* parameter. Which is obvious due to the smaller ionic size of Al. The C substitution which goes to the Boron Plane also affects the c parameter. For 1% it jumps high a little and decreases further with increase of doping. It has been reported earlier that C alone does not affect the *c* lattice parameter. But here with Al co doping the C causes to affect the *c* lattice parameter also. But the main point here is that the *c* increases for 1% of C.
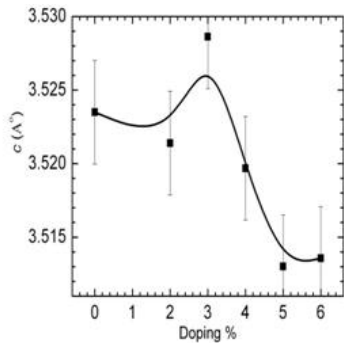

Fig. 5. *c* parameter of Al-C co-doped $Mg_{1-x}Al_x(B_{1-y}C_y)_2$ superconductors as function of total doping % C and Al.
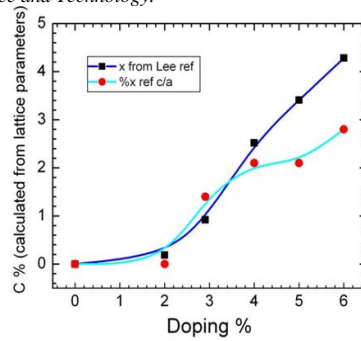

Fig. 6. *% of C* doping in Al-C co-doped $Mg_{1-x}Al_x(B_{1-y}C_y)_2$ superconductors as function of total doping % C and Al. This has been calculated from the lattice parameters. ■ – calculated from *a* parameter's of C-doped single crystals as provided by S. Lee et al. ● calculated from the c/a ratio using $x= 7.5*\Delta(c/a)$

The C substitution is estimated from change in lattice parameter which is shown in Figure 6. We used the decrease of *a* parameter of C doped single crystal MgB_2 of S. Lee data as standard. Also we use the formula $x= 7.5*\Delta(c/a)$ of Avdeev et al to calculate the doping concentration. From figure 6 it is obvious that the standard taken from S lee data gives the better matching. In Al-C co doping both parameters is changing while in C doping only *a* parameter is changing and *c* remains constant.

It has been reported earlier that C alone does not affect the *c* lattice parameter. But here with Al co doping the C causes to affect the *c* lattice parameter also as shown in Fig. 5. But the main point here is that the *c* increases for 1% of C.

The graph of Tc and ρ_0 Figure 8, 9 as function of doping concentration from resistivity measurement clearly shows that the plateau region around 1 to 3% of C and 2% of Al divided in two region. The drop in Tc is faster in the first region in compared to that of 2nd region while ρ_0 has reverse behavior.
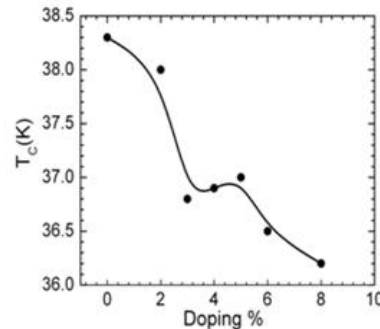

Fig.8. T_C of Al-C co-doped $Mg_{1-x}Al_x(B_{1-y}C_y)_2$ superconductors as function of combined % of C and Al.
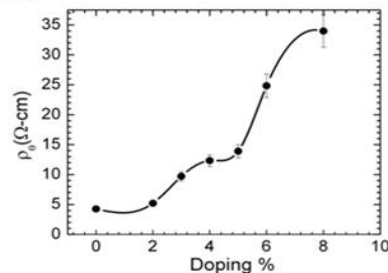

Fig.9. ρ_0 of Al-C co-doped $Mg_{1-x}Al_x(B_{1-y}C_y)_2$ superconductors as function of combined % of C and Al.

M-H loop is show in Fig 10. Jc is calculated using Bean's Critical State Model is shown in Fig. 11, 12. It is obvious that the Jc in Al 2% and C1% doped sample has the highest Jc in all range of field. Jc has been increased by one order at 4.5 T in comparison to pure sample. Our earlier study of Al doping has shown the highest Jc in 2% of doping here we achieve even higher than that with addition of C.
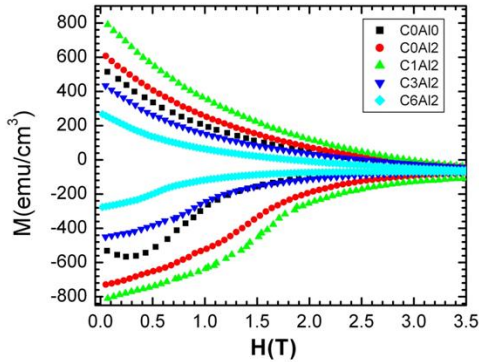

Fig.10. Magnetization of Al-C co-doped $Mg_{1-X}Al_X(B_{1-y}C_y)_2$ superconductors as function of magnetic field.
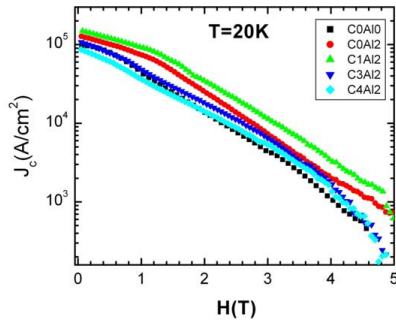

Fig.11. Jc of Al-C co-doped $Mg_{1-X}Al_X(B_{1-y}C_y)_2$ superconductors as function of magnetic field.
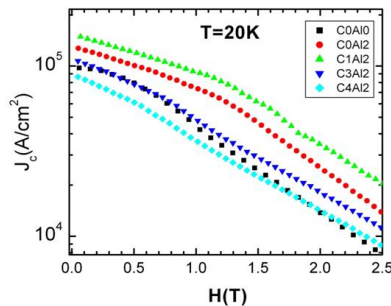

Fig. 12. Jc of Al-C co-doped $Mg_{1-X}Al_X(B_{1-y}C_y)_2$ superconductors as function of magnetic field

CONCLUSION

In Summary, result shows the substitution of nano carbon and alumina doped in the stoichiometry of MgB_2. The impurity MgO, as seen in the XRD plot, might arise during the solid-state reaction of the starting materials. The variation in *delta Tc* value and transition temperature, T_c is perceived with the increase of doping concentration. Slight variation in T_c (onset) and T_c ($\rho = 0$) is observed from the temperature dependence of resistivity plot for nano carbon and alumina doped MgB_2. The Full Widths at Half Maximum (FWHM) showing higher value in 102 peak and lower value in 100 peak. The XRD and resistivity measurements clearly show that there is remarkable change around 1% of C and 2% Al doping which has been manifested as the highest Jc at that

point in the all range of field. Thus we achieved the enhancement of Jc of MgB_2 by co-doping in comparison to the individual doping of Al and C at 20K.

REFERENCES

[1] J. Nagamatsu, N. Nakagawa, T. Muranaka, J. Akimitsu, Nature 410 (2001) 63.

[2] M. Paranthaman, J.R. Thompson, D.K. Christen, Physica C 355 (2001) 1.

[3] J.S. Ahn, E.J. Choi, cond-mat/0103169.

[4] T. Takenobu, T. Ito, D.H. Chi, K. Prassides, Y. Iwasa, Phys. Rev. B 64 (2001) 134513.

[5] [W. Mickelson, J. Cumings, W.Q. Han, A. Zettl, Phys. Rev. B 65 (2002) 052505.

[6] Z.-h. Cheng, B.-g. Shen, J. Zhang, S.-y. Zhang, T.-y. Zhao, H.-w. Zhao, J. Appl. Phys. 91 (2002) 7125.

[7] A. Bharathi , S. Jemina Balaselvi, S. Kalavathi, G.L.N. Reddy, V. Sankara Sastry, Y. Hariharan, T.S. Radhakrishnan, Physica C 370 (2002) 211.

[8] M. Kazakov et.al, cond-mat/103350

[9] S.X. Dou, S. Soltanian, J. Horvat, X.L. Wang, S.H. Zhou, M. Ionescu, H.K. Liu, Appl. Phys. Lett. 81 (2002) 3419.

[10] B.J. Senkowicz, J.E. Giencke, S. Patnaik, C.B. Eom, E.E. Hellstrom, D.C. Larbalestier, Appl. Phys. Lett. 86 (2005) 202502.

[11] J.H. Lim, K.T. Kim, E.C. Park, C.M. Lee, J.H. Shim, J. Joo, W.N. Kang, C. Kim, Physica C 468 (2008) 1379.

[12] S.X. Dou, W.K. Yeoh, J. Horvat, M. Ionescu, Appl. Phys. Lett. 83 (2003) 4996.

[13] J.S. Slusky, N. Rogado, K.A. Regan, M.A. Hayward, P. Khalifah, T. He, K. Inumaru, S.M. Loureiro, M.K. Hass, H.W. Zandbergen, R.J. Cava, Nature 410 (2001) 343.

[14] J. Kortus, O.V. Dolgov, R.K. Kremer, Phys. Rev. Lett. 94 (2005) 027002.

[15] X.F. Rui et al. / Physica C 412–414 (2004) 312–315

[16] Intikhab A. Ansari, M. Shahabuddin, Khalil A Ziq, A. F. Salem, V.P.S. Awana, M. Husain and H. Kishan 2007 *Supercond. Sci. Technol.* **20** 827.